

Calabi–Yau Metrics with Full Moduli Dependence

Andrei Constantin^{a,b,1}, Seung-Joo Lee^{c,2}, Andre Lukas^{b,3}, Luca A. Nutricati^{b,4}

^a *School of Mathematics, University of Birmingham
Watson Building, Edgbaston, Birmingham B15 2TT, UK*

^b *Rudolf Peierls Centre for Theoretical Physics, University of Oxford
Parks Road, Oxford OX1 3PU, UK*

^c *Department of Physics, Yonsei University
Seoul 03722, Republic of Korea*

Abstract

Recent advances in numerical and machine-learning methods have enabled highly accurate constructions of Ricci-flat metrics on compact Calabi–Yau three-folds. For phenomenological applications it is crucial to understand how these metrics vary across moduli space. In this work, we construct approximate analytic expressions for Ricci-flat Calabi–Yau metrics with explicit complex-structure and Kähler moduli dependence by combining machine-learned numerical data with symbolic regression. Our approach is based on an explicit Ansatz for the Kähler potential with moduli-dependent coefficients. Fitting this Ansatz to numerical data and applying symbolic regression allows us to reconstruct analytic formulae for these coefficients, thereby obtaining approximate Ricci-flat metrics with explicit moduli dependence. We apply the construction to a one-parameter family of bi-cubic three-folds in $\mathbb{P}^2 \times \mathbb{P}^2$, achieving percent-level agreement with the underlying numerical data.

¹a.constantin@bham.ac.uk

²seungjoolee@yonsei.ac.kr

³andre.lukas@physics.ox.ac.uk

⁴luca.nutricati@physics.ox.ac.uk

1 Introduction

One of the oldest ambitions of string phenomenology is to derive the couplings and masses of low-energy effective theories from the geometry and moduli of the extra dimensions rather than treating them as input data. Over the past few years substantial progress has been made in this direction. Numerical and machine-learning methods now make it possible to approximate Ricci-flat metrics on compact Calabi–Yau (CY) manifolds well enough to feed them into concrete physical calculations, including calculations of physical Yukawa couplings and fermion masses in heterotic compactifications [1–3]. Since these observables vary across moduli space, the numerical determination of Ricci-flat metrics must be repeated at many different points in moduli space.

Many quantities relevant for phenomenology are determined by topological or quasi-topological data. Physical couplings, however, also depend on wave-function normalisation factors and therefore require detailed metric information. Although these computations can now be carried out using numerical techniques [4–16], purely numerical representations have intrinsic limitations. Numerical methods, such as neural networks trained at a fixed point in moduli space, provide an approximation to the quantities of interest, but not explicit analytic expressions. As a result, important geometrical structures underlying the relation between moduli and low-energy physics may remain hidden. Moreover, numerical representations are difficult to extrapolate and cumbersome to differentiate with respect to the moduli in a controlled manner.

Despite their importance, explicit analytic Ricci-flat metrics are largely unavailable for compact Calabi–Yau three-folds. While remarkable constructions exist for K3 surfaces, where hyperkähler geometry and instanton methods have led to analytic descriptions of Ricci-flat metrics [17, 18], no comparable analytic description is currently known for compact Calabi–Yau three-folds.

The purpose of this article is to combine and extend the approaches developed in Refs. [19, 20]. These complementary works construct approximate Ricci-flat CY metrics in analytic form with explicit dependence on complex-structure and Kähler moduli, respectively. The former focuses on complex-structure dependence, while the latter develops a framework that accommodates explicit Kähler-moduli dependence for manifolds with $h^{1,1}(X) > 1$. Here we unify these approaches to construct approximate Ricci-flat metrics with simultaneous dependence on both complex-structure and Kähler moduli. Although the method is general, we illustrate it using a one-parameter family of bi-cubic three-fold hypersurfaces in $\mathbb{P}^2 \times \mathbb{P}^2$.

2 From numerical metrics to analytic formulae

Symbolic expressions for approximate Ricci-flat Kähler potentials on CY manifolds with explicit moduli dependence have been constructed in Refs. [19, 20]. Here we combine these approaches to obtain analytic approximations that depend simultaneously on both complex-structure and Kähler moduli. For

mathematical background on Kähler geometry and manifolds with special holonomy see, for example, Ref. [21].

Our starting point is an analytic Ansatz for the Kähler potential containing a finite set of free parameters. Ricci-flat metric data are generated numerically at a collection of points in the combined complex-structure and Kähler moduli space using the `cymetric` package [14]. The parameters of the Ansatz are then determined by fitting to these data at each point in moduli space. Finally, symbolic regression is applied to the resulting parameter values in order to reconstruct their dependence on the moduli analytically.

Building a suitable Ansatz. Before writing down the Ansatz, let us briefly set up the basic framework and the notation. Consider a CY hyper-surface X embedded in an ambient space \mathcal{A} which, for simplicity, we take to be a product of complex projective spaces⁵, $\mathcal{A} = \prod_{r=1}^m \mathbb{P}^{n_r}$ with homogenous coordinates

$$x = \left(x_1^{(1)}, \dots, x_{n_1+1}^{(1)}, \dots, x_1^{(m)}, \dots, x_{n_m+1}^{(m)} \right). \quad (2.1)$$

Kähler classes $[J]$ on X can be parametrised as

$$[J] = \sum_{r=1}^{h^{1,1}(X)} t_r [J_r] \in H^{1,1}(X, \mathbb{R}), \quad (2.2)$$

where the $[J_r]$ form a basis of $H^{1,1}(X, \mathbb{R})$ and t_r are the Kähler moduli, collectively denoted by $t = (t_1, \dots, t_{h^{1,1}(X)})$. In the case of favourable embeddings, which will be our focus throughout this paper, $m = h^{1,1}(X)$ and the basis elements $[J_r]$ can be chosen as the restrictions of the ambient-space hyperplane classes. Complex structure moduli will be denoted as $\psi = (\psi_1, \dots, \psi_{h^{2,1}(X)})$.

Following Ref. [20] we write the Ricci-flat Kähler potential as a Fubini–Study piece plus a globally defined correction,

$$K(x, \psi, t) = K_{\text{FS}}(x, \psi, t)|_X + \phi(x, \psi, t) \quad (2.3)$$

where the ambient-space Fubini–Study Kähler potential

$$K_{\text{FS}}(x, \psi, t) = \sum_{r=1}^m \frac{t_r}{\pi} \log \left(\sum_{a=0}^{n_r} |x_a^{(r)}|^2 \right) \quad (2.4)$$

has been restricted to the CY manifold. Although the complex-structure moduli do not appear explicitly in Eq. (2.4), they enter through the restriction to the hypersurface X . Since all evaluations are performed on sampled points of the CY manifold, this implicit dependence presents no practical difficulties.

The Ansatz for the globally defined function ϕ is built from a finite-dimensional space of sections of an ample line bundle $L = \mathcal{O}_X(k)$, where $k = (k_1, \dots, k_m)$, and $(s_I)_{I=1, \dots, h^0(X, L)}$ denotes a basis of global

⁵The method can be easily generalised to CY manifolds defined as hyper-surfaces or complete intersections in more general toric ambient spaces.

holomorphic sections of L . Specifically, the Ansatz reads

$$\phi(x, \psi, t) = V(t)^{1/3} \frac{\sum_{I,J} \alpha_{IJ}(\psi, t_1/t_m, \dots, t_{m-1}/t_m) s_I(x) \overline{s_J(x)}}{\prod_{r=1}^m \left(\sum_{a=0}^{n_r} |x_a^{(r)}|^2 \right)^{k_r}}, \quad (2.5)$$

where the CY volume factor $V(t) = \frac{1}{3!} \int_X J^3$ has been introduced to ensure the correct scaling of the metric under a rescaling of the Kähler parameters $t_r \rightarrow \lambda t_r$.

Generalising the construction of Ref. [20], the coefficients α_{IJ} are taken to depend on both the complex-structure moduli ψ and the Kähler moduli ratios t_i/t_m for $1 \leq i \leq m-1$. Since ϕ is globally defined, it does not modify the Kähler class, so the Kähler class associated to K is entirely determined by the Fubini–Study contribution and is parametrised by Eq. (2.2). For each point in moduli space, the coefficients α_{IJ} will be determined by fitting the Ansatz to numerical Ricci-flat metric data obtained from machine learning. As usual, increasing the degree k enlarges the space of sections and is expected to improve the accuracy of the Ansatz.

The role of discrete symmetries. In the following analysis we require that the CY hypersurfaces under consideration admit a large discrete symmetry. This symmetry is reflected at the level of the metric and the Kähler potential and is used in order to simplify the structure of the Ansatz. (See Refs. [19, 20] for an argument establishing the fact that a holomorphic automorphism of a CY manifold is respected by the Ricci-flat metric.)

Retrieving analytic results. Given the analytic Ansatz discussed above, we first use neural networks to learn the Ricci-flat Kähler potential numerically on a grid in moduli space and determine the corresponding Ansatz coefficients by fitting to the learned data. We then apply symbolic regression, implemented with PySR [22], to reconstruct explicit moduli-dependent expressions for these coefficients. This yields an approximate analytic formula for the Ricci-flat Kähler potential with explicit full moduli dependence.

3 The bi-cubic three-fold

3.1 Geometry and conventions

To set the stage, let us consider bi-cubic three-folds X defined as hypersurfaces in the ambient space $\mathbb{P}^2 \times \mathbb{P}^2$. We denote the homogeneous coordinates on the two projective factors by x_a and y_a , respectively, where $a = 0, 1, 2$. On the patch $x_0 \neq 0$, $y_0 \neq 0$, one may use the affine coordinates x_a/x_0 and y_a/y_0 with $a = 1, 2$. The manifold X is defined as the zero locus of a polynomial P of bi-degree $(3, 3)$ and has Hodge numbers

$$(h^{1,1}(X), h^{2,1}(X)) = (2, 83).$$

The Kähler class can be written as

$$[J] = t_1[J_1] + t_2[J_2],$$

where $[J_1]$ and $[J_2]$ are the restrictions to X of the Fubini–Study classes on the two ambient projective-space factors. Relative to this basis, the Kähler cone is characterised by $t_1, t_2 > 0$, and the volume is

$$V(t_1, t_2) = \frac{3}{2} t_1 t_2 (t_1 + t_2).$$

There exist families of bi-cubics with large discrete symmetry groups that considerably simplify the analysis. We now describe one such family.

3.2 Symmetry-reduced Ansatz

The generators of the symmetry group under consideration act linearly on the homogeneous coordinates as

$$\begin{aligned} (\mathbb{Z}_3^{(x)})_a &: x_a \mapsto \omega x_a \quad , \quad x_b \mapsto x_b \text{ for } b \neq a, \quad y_c \mapsto y_c \text{ for } c = 0, 1, 2 \\ (\mathbb{Z}_3^{(y)})_a &: y_a \mapsto \omega y_a \quad , \quad y_b \mapsto y_b \text{ for } b \neq a, \quad x_c \mapsto x_c \text{ for } c = 0, 1, 2 \\ S_3^{(x,y)} &: x_a \mapsto x_{\sigma(a)} \quad , \quad y_a \mapsto y_{\sigma(a)} \text{ where } \sigma \in S_3 \\ \mathbb{Z}_2^{(x,y)} &: x_a \mapsto y_a \quad , \quad y_a \mapsto x_a \text{ for } a = 0, 1, 2 \end{aligned} \tag{3.1}$$

where $\omega = e^{2\pi i/3}$. Note that the generators in the first three lines act trivially on the Kähler moduli, while the last one exchanges the two moduli, $t_1 \leftrightarrow t_2$. To obtain the induced projective symmetry group, one must quotient by the two diagonal \mathbb{Z}_3 actions $x_a \mapsto \omega x_a, y_a \mapsto y_a$ and $x_a \mapsto x_a, y_a \mapsto \omega y_a$, with $a = 0, 1, 2$, which are part of the projective rescalings of the two ambient \mathbb{P}^2 factors. The resulting projective symmetry group is

$$G \cong \left((\mathbb{Z}_3^{(x)})^2 \times (\mathbb{Z}_3^{(y)})^2 \right) \rtimes (S_3 \times \mathbb{Z}_2), \tag{3.2}$$

of order $|G| = 3^4 \cdot 6 \cdot 2 = 972$. The most general bi-cubic defining polynomial invariant under this symmetry group is

$$P = P_1 + \psi P_2, \quad P_1 = \sum_a x_a^3 y_a^3, \quad P_2 = \sum_{a \neq b} x_a^3 y_b^3, \tag{3.3}$$

where ψ is the single remaining complex-structure modulus.

The bi-cubic three-folds defined as the zero locus of P become singular when $\psi = -\frac{1}{2}, 0, \pm 1, \infty$ and are smooth otherwise. Of the five values of the parameter, $\psi = -\frac{1}{2}, -1$ and ∞ each leads to a finite number of point-like singularities on the bi-cubic hypersurface, while $\psi = 0$ and $\psi = 1$ correspond to severer singular loci of complex dimensions one and two, respectively.

Our next step is to specialise the Kähler potential Ansatz in Eq. (2.3) to the above one-parameter family of bi-cubics. We choose the line bundle $L = \mathcal{O}_X(2, 2)$ whose sections form a space of dimension

$h^0(X, L) = 36$. This means that the hermitian matrix α_{IJ} in the Ansatz (2.3) is of size 36×36 and, hence, contains 1296 real parameters. Consequently, for a general bi-cubic this is a rather complicated problem. However, for the one-parameter family in Eq. (3.3) the sections combine into only eight quantities I_i , explicitly defined below, with well-defined transformation properties under G . In terms of these quantities, the Ansatz (2.3) takes the form

$$\phi(x, \psi, t_1, t_2) = V(t_1, t_2)^{1/3} \sum_{i=0}^7 \alpha_i \left(\psi, \frac{t_1}{t_2} \right) \frac{I_i(x, y)}{(\sum_A |x_A|^2)^2 (\sum_A |y_A|^2)^2}. \quad (3.4)$$

The coefficients α_i depend on the complex structure parameter ψ and the one ratio, t_1/t_2 , of Kähler parameters and will be determined by our fit to the data. The factor $V^{1/3}$ ensures the correct homogeneity under an overall rescaling of the Kähler class. The quantities I_i are invariants of the subgroup of G that preserves the Kähler structure. This subgroup is generated by all transformations in Eq. (3.1) except for the $\mathbb{Z}_2^{(x,y)}$ symmetry in the last line, which exchanges the two Kähler parameters t_1 and t_2 . Explicitly, the invariants are given by

$$\begin{aligned} I_0 &= \sum_{a < b} |x_a|^2 |x_b|^2 |y_a|^2 |y_b|^2, & I_1 &= \sum_{\substack{a \neq b, c \\ b < c}} |x_a|^4 |y_b|^2 |y_c|^2, \\ I_2 &= \sum_{a \neq b} |x_a|^4 |y_a|^2 |y_b|^2, & I_3 &= \sum_{a \neq b} |x_a|^4 |y_b|^4, \\ I_4 &= \sum_a |x_a|^4 |y_a|^4, & I_5 &= \sum_{a, b, c \text{ distinct}} |x_a|^2 |y_a|^2 |x_b|^2 |y_c|^2, \\ I_6 &= \sum_{a \neq b} |y_a|^4 |x_a|^2 |x_b|^2, & I_7 &= \sum_{\substack{a \neq b, c \\ b < c}} |y_a|^4 |x_b|^2 |x_c|^2. \end{aligned} \quad (3.5)$$

The action of $\mathbb{Z}_2^{(x,y)}$ leaves I_i invariant for $i = 0, 3, 4, 5$, while it exchanges $I_1 \leftrightarrow I_7$ and $I_2 \leftrightarrow I_6$. Consequently, the coefficients α_i satisfy

$$\begin{aligned} \alpha_1(\psi, t_{12}) &= \alpha_7(\psi, t_{21}), & \alpha_2(\psi, t_{12}) &= \alpha_6(\psi, t_{21}), \\ \alpha_i(\psi, t_{12}) &= \alpha_i(\psi, t_{21}), & & \text{for } i = 0, 3, 4, 5, \end{aligned} \quad (3.6)$$

where $t_{12} \equiv t_1/t_2 = t_{21}^{-1}$. These relations provide non-trivial consistency checks on the coefficients extracted from the numerical data.

3.3 Results

For the numerical calculation of Ricci-flat metrics we consider bi-cubics defined as zero loci of the polynomial P in Eq. (3.3) for the moduli space points

$$\left\{ (\psi, t_1, t_2) \left| \begin{array}{l} \psi = m + in, \text{ with } m, n = -4, \dots, 5, \text{ and } \psi \neq 0, \pm 1 \\ V(t_1, t_2) = 40, \frac{t_1}{t_2} = \frac{1}{11}, \frac{1}{9}, \frac{1}{7}, \frac{2}{11}, \frac{3}{13}, \frac{3}{10}, \frac{5}{13}, \frac{1}{2}, \frac{8}{13}, \frac{11}{14}, 1, \dots \end{array} \right. \right\} \quad (3.7)$$

where, in the case of the Kähler moduli, the dots indicate the inclusion of all the reciprocals. These constitutes a total of $97 \times 21 = 2037$ points in the full moduli space. Note, we have excluded the values of ψ where the manifold becomes singular. For each of these points in moduli space we sample $N = 200,000$ points on the corresponding bi-cubic, using the `cymetric` point generator, and then learn the Ricci-flat Kähler potential with the `cymetric` ϕ -model. Fitting to this data, the coefficients $\alpha_i(\psi, t_{12})$ in the Ansatz Eq. (3.4) are then determined for each of the values (ψ, t_{12}) in Eq. (3.7). Finally, symbolic regression is applied to these results in order to find symbolic expressions for $\alpha_i(\psi, t_{12})$.

Fig. 1 summarises the accuracy of the construction. In the left panel we show the σ -loss for both the neural-network metric and the analytic metric obtained via symbolic regression. The σ -loss measures the extent to which the predicted metric satisfies the Monge–Ampère equation and is defined by

$$\sigma_{\text{loss}} = \frac{1}{N} \left\| 1 - \frac{\det g_{\text{pr}}}{\kappa \Omega \wedge \bar{\Omega}} \right\|_1, \quad (3.8)$$

where g_{pr} denotes the predicted Ricci-flat metric, Ω is the holomorphic $(3,0)$ form, κ is a moduli-dependent constant, and the L_1 norm is evaluated over a sample of N points on the manifold. Thus, σ_{loss} corresponds to the average pointwise deviation from the Monge–Ampère equation. In the right panel we show the average percentage deviation of the analytic Kähler potential K from its neural-network counterpart K_{NN} . Results are displayed for three representative values of the complex-structure modulus. The observed accuracy depends only weakly on this parameter.

The σ -loss of the numerical metric demonstrates that the neural network is able to learn Ricci-flat metrics with good accuracy throughout the range of Kähler parameters considered. Although the σ -loss of the analytic metric is larger than that of the corresponding neural-network solution, it remains sufficiently small for the analytic metric to provide a good approximation to a Ricci-flat metric.

Applying symbolic regression to the numerical values of the coefficients $\alpha_i(\psi, t_{12})$ yields explicit analytic expressions for their dependence on both the complex-structure and Kähler moduli. Fig. 2 compares these analytic expressions with the corresponding coefficient values extracted from the numerical fits. The analytic results are shown as red surfaces, while the fitted numerical values are represented by blue points. For clarity, the figure displays four representative coefficients and restricts the complex-structure dependence to fixed slices in the ψ -plane.

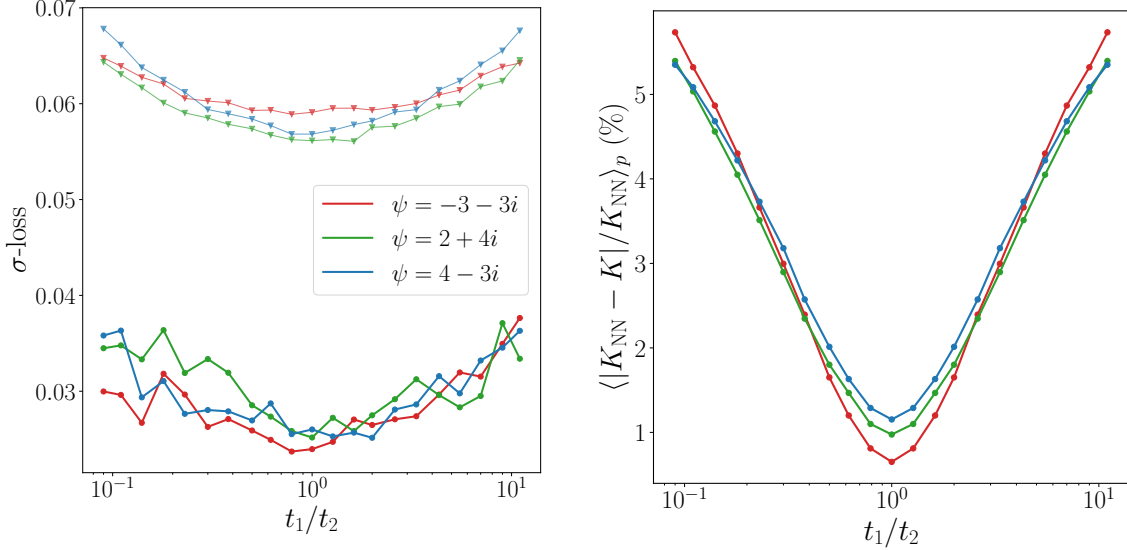


Figure 1: Left: Comparison of the σ -loss computed from the analytical expression obtained via symbolic regression (triangles) and that obtained by the neural network after training (circles), for all considered values of the ratio t_1/t_2 . Results are shown for three different values of the complex structure parameter. Right: Percentage deviation $\langle |K_{\text{NN}} - K|/K_{\text{NN}} \rangle$, averaged over N sampled points on the manifold, as a function of t_1/t_2 for the same values of the complex structure parameter. Averaged over the moduli, the σ -loss and the deviation of the potential are 0.06 and 3.2%, respectively.

The top-left panel of Fig. 2 shows the results for α_1 . The plot is truncated at $\Re(\psi) = 0$, as the singularity of the manifold at $\psi = 0$ is reflected in the corresponding symbolic-regression expression, which becomes singular at that point. Indeed, this singularity at $\psi = 0$ appears in almost all the other coefficient expressions. However, despite its severity, the manifold singularity at $\psi = 1$ corresponds to a regular point of the symbolic-regression expression for all the coefficients. At present, we do not know of a theoretical reason why singularities of the manifold should necessarily be reflected in the coefficients of the Kähler potential. The singularity at $\psi = 0$ may therefore be an artefact of the symbolic-regression procedure. Clarifying this issue would require a more detailed analysis based on denser sampling near the singular loci, which lies beyond the scope of the present work.⁶

The lower panels of Fig. 2 already suggest that α_3 and α_4 satisfy the symmetry properties implied by Eq. (3.6). These relations become more apparent in Fig. 3, where the fitted coefficient values are shown as functions of t_1/t_2 for fixed ψ . The corresponding analytic expressions obtained from symbolic

⁶Of the two singular members with $\psi = 0$ and $\psi = 1$ that exhibit severe singularities, the $\psi = 1$ case is already in the standard form, degenerating into the union of two smooth non-CY components intersecting normally along a surface. Similar normal-crossing degenerations arise for the one-parameter families of quintics and bi-cubics studied in Ref. [19], in the large-complex-structure limits thereof; note that, for the members with fairly large ψ values of those two families, the analytic approximation based on the ϕ -model was observed to reproduce the numerically determined Ricci-flat Kähler potential to within a few percent.

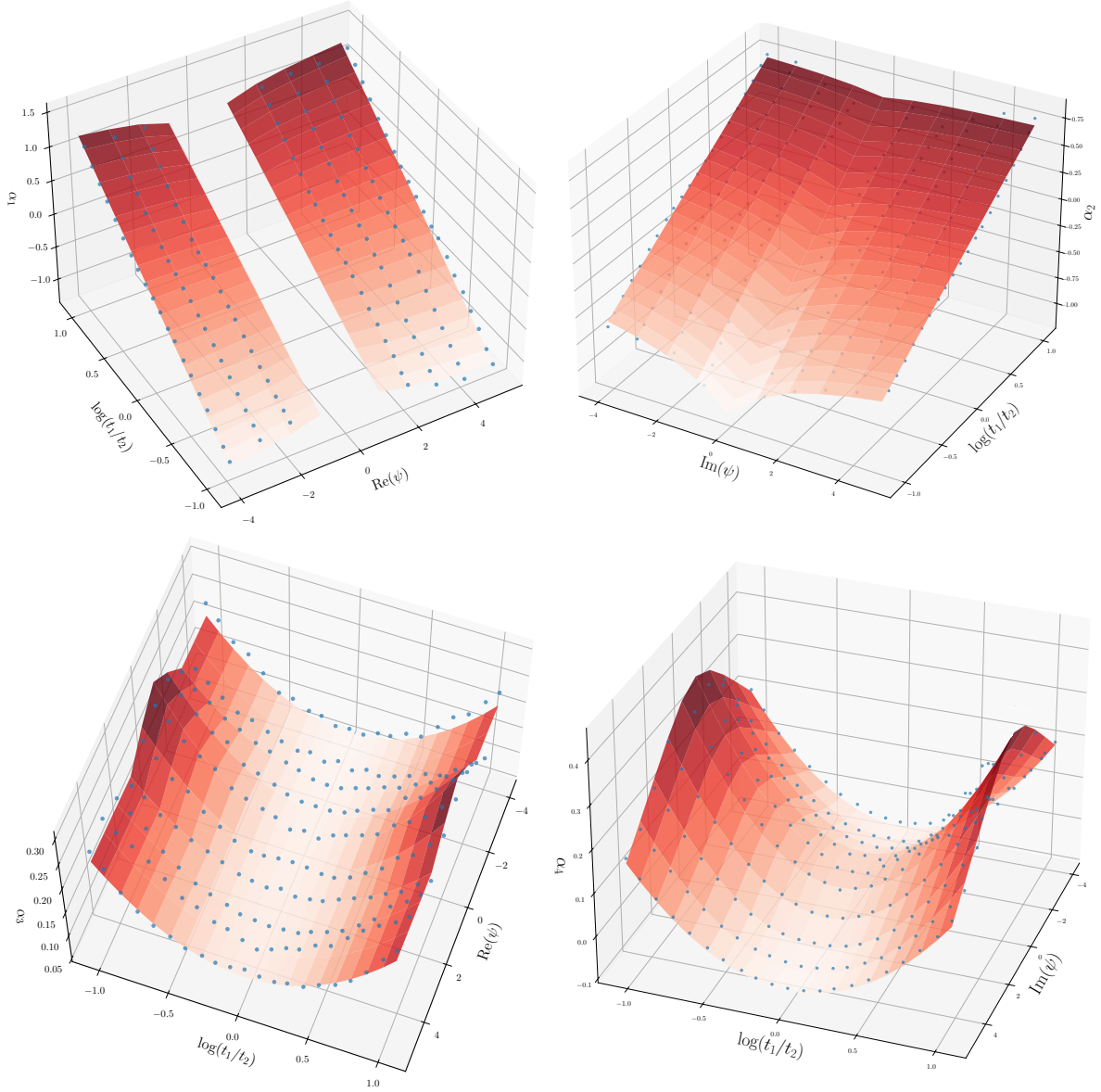


Figure 2: Three-dimensional plots of the first four coefficients α_i as functions of t_1/t_2 , shown on representative slices of the complex-structure moduli space. The blue points denote the coefficient values obtained from fits to the numerical data, while the red surfaces show the corresponding analytic expressions derived via symbolic regression. In the left panels, $\Im(\psi)$ is fixed to 0 and 2 (from top to bottom), whereas in the right panels, $\Re(\psi)$ is fixed to -1 and -2 . The truncation visible in the top-left panel is caused by a singularity at $\psi = 0$ in the symbolic-regression expression.

regression are shown as black curves. Substituting these analytic expressions into Eq. (3.4) yields the following explicit analytic approximation to the Ricci-flat Kähler potential, with full dependence on both the complex-structure and Kähler moduli, as written in Eq. (3.9).

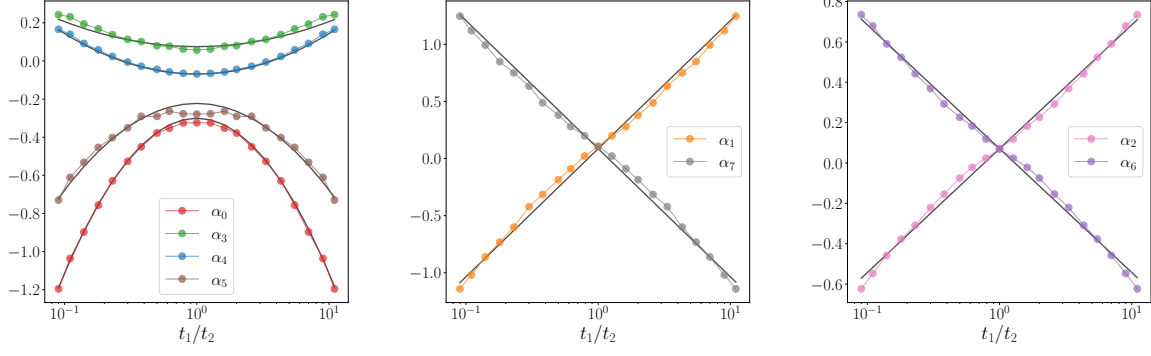


Figure 3: Best-fit numerical values of the coefficients α_i as functions of the moduli ratio t_1/t_2 for fixed values of ψ . The corresponding analytical expression obtained using symbolic regression is plotted as a black line.

$$\begin{aligned}
K(x, \psi, t_1, t_2) = & K_{\text{FS}}|_X + \frac{V(t_1, t_2)^{1/3}}{(\sum_A |x_A|^2)^2 (\sum_A |y_A|^2)^2} \left\{ \right. \\
& \left[-0.3 - 0.07 \log(0.38 |\psi|^2) \log^2(t_{12}) \right] \sum_{a < b} |x_a|^2 |x_b|^2 |y_a|^2 |y_b|^2 \\
& + (0.38 + 0.037 \log |\psi|^2)(0.18 + \log t_{12}) \sum_{\substack{a \neq b, c \\ b < c}} |x_a|^4 |y_b|^2 |y_c|^2 \\
& + (t_{12} \rightarrow t_{21}, x \leftrightarrow y) \\
& + \left[\log(|\psi|^2) + 0.85 \Re \psi \right] (0.064 - 0.002 \log t_{12}) + 0.32 \log t_{12} - 0.1 \left. \right] \sum_{a \neq b} |x_a|^4 |y_a|^2 |y_b|^2 \\
& + (t_{12} \rightarrow t_{21}, x \leftrightarrow y) \\
& + \left[0.08 + (0.024 + 0.014 e^{-0.564(\Re \psi)^4}) \log^2(t_{12}) \right] \sum_{a \neq b} |x_a|^4 |y_b|^4 \\
& + \left[(0.07 - 0.001(|\psi|^2 - 0.28 \Im \psi))(1.5 - \log |\psi|^2 + \log^2(t_{12})) \right] \sum_a |x_a|^4 |y_a|^4 \\
& - \left[0.22 + 0.02 \log((\Im \psi)^2 + 3.71(\Re \psi)^2) \left(e^{-0.46\Re \psi + 0.13(\Re \psi)^2} + \log^2(t_{12}) \right) \right] \sum_{a, b, c \text{ distinct}} |x_a|^2 |y_a|^2 |x_b|^2 |y_c|^2 \left. \right\} \tag{3.9}
\end{aligned}$$

As before, we note that the Fubini–Study contribution is restricted to the CY manifold. As a result, it acquires an implicit dependence on the complex-structure parameter ψ through the defining polynomial from Eq. (3.3). As stated above, the associated σ -loss and average percentage deviation from the numerical Kähler potential are 0.06 and 3.2%, respectively. We emphasise that this level of accuracy is achieved already for $k = (k_1, k_2) = (2, 2)$, corresponding to a relatively low-degree line bundle. A

noteworthy outcome of our analysis is that accurate analytic approximations do not require large values of k ; the essential geometric features are already captured by a comparatively simple Ansatz.

4 Conclusions and outlook

In this paper, we have developed a method for constructing approximate Ricci-flat Kähler potentials with explicit dependence on both complex-structure and Kähler moduli. The construction combines numerical Ricci-flat metric data with a suitable analytic Ansatz for the Kähler potential, based on sections of a line bundle $L = \mathcal{O}_X(k)$, together with symbolic regression. We have implemented this approach for a one-parameter family of bi-cubic CY hypersurfaces in $\mathbb{P}^2 \times \mathbb{P}^2$, but the method is sufficiently general to be applied to a broad class of CY manifolds, including hypersurfaces and complete intersections in toric ambient spaces.

Although our results only provide approximately Ricci-flat metrics we still anticipate meaningful applications in the context of CY string compactifications. As mentioned, in such compactifications, the physically relevant quantities depend on both complex-structure and Kähler parameters. Having metrics available which display the dependence on these moduli explicitly, allows for ‘tracking’ the value of physical quantities across the moduli space. The approximate nature of our results is not necessarily prohibitive in this context. Most string calculations, certainly at the level of physical models, are carried out using various approximations, including the α' and loop expansions of string theory. The approximate nature of our results simply provides another contribution to the inevitable error in such calculations. As to the size of this error, it is instructive to note that the calculation of Yukawa couplings performed in Ref. [2] shows that using a Fubini-Study metric (that is, the first term in the Ansatz (2.3) only) leads to quark and lepton masses that deviate by only about 20% from those obtained with a machine-learned Ricci-flat metric. Our result is a very significant improvement on merely considering the Fubini-Study metric which suggests it may lead Yukawa couplings with percent level errors.

There are various extensions of the present work. First, one might attempt to carry out the programme described in this paper for more complicated CY manifolds and/or higher-dimensional moduli spaces. There are several versions of this goal. The most conservative is to remain within highly symmetric families and enlarge the parameter space gradually, adding one modulus at a time. A more ambitious version would treat several complex-structure and several Kähler moduli simultaneously, perhaps with sparse sampling combined with stronger inductive biases at the symbolic-regression stage.

In view of calculating physical quantities it seems desirable to extend the present philosophy to the additional geometric ingredients entering such calculations. For example, it might well be possible to obtain approximate analytic results for Hermitian Yang–Mills connections on bundles, and harmonic forms.

An important direction for future work is to determine how large the line bundle degree must be in

order for the analytic metric to achieve a level of Ricci-flatness comparable to that of the numerical solution. While the analytic metric already provides a good approximation to a Ricci-flat metric, it remains an open question whether increasing the degree of the associated line bundle can systematically reduce the remaining discrepancy.

Finally, a natural question is why one should employ a neural network to learn the Ricci-flat Kähler potential when, in principle, the analytic metric itself could be learned directly using symbolic regression with a loss function enforcing Ricci-flatness. While this certainly represents an interesting direction for future investigation, there are indications that such an approach may be computationally prohibitive [23].

Acknowledgements

AC and LAN are supported by the Royal Society grant DHF/R1/231142. AL is supported by the STFC consolidated grant ST/X000761/1. The work of SJL is supported by the Yonsei University Research Fund 2026-22-0183.

References

- [1] Giorgi Butbaia, Damián Mayorga Peña, Justin Tan, Per Berglund, Tristan Hübsch, Vishnu Jejjala, and Challenger Mishra. “Physical Yukawa couplings in heterotic string compactifications”. In: *Adv. Theor. Math. Phys.* 28.8 (2024), pp. 2783–2822. DOI: 10.4310/atmp.241119041341. arXiv: 2401.15078 [hep-th].
- [2] Andrei Constantin, Cristoforo S. Fraser-Taliente, Thomas R. Harvey, Andre Lukas, and Burt Ovrut. “Computation of quark masses from string theory”. In: *Nucl. Phys. B* 1010 (2025), p. 116778. DOI: 10.1016/j.nuclphysb.2024.116778. arXiv: 2402.01615 [hep-th].
- [3] Per Berglund, Giorgi Butbaia, Tristan Hübsch, Vishnu Jejjala, Damián Mayorga Peña, Challenger Mishra, and Justin Tan. “Precision string phenomenology”. In: *Phys. Rev. D* 111.8 (2025), p. 086007. DOI: 10.1103/PhysRevD.111.086007. arXiv: 2407.13836 [hep-th].
- [4] S. K. Donaldson. “Some numerical results in complex differential geometry”. In: *Pure Appl. Math. Q.* (2009), pp. 571–618. DOI: 10.4310/PAMQ.2009.v5.n2.a2.
- [5] Michael R. Douglas, Robert L. Karp, Sergio Lukic, and Rene Reinbacher. “Numerical Calabi-Yau metrics”. In: *J. Math. Phys.* 49 (2008), p. 032302. DOI: 10.1063/1.2888403. arXiv: hep-th/0612075.
- [6] Volker Braun, Tamaz Brelidze, Michael R. Douglas, and Burt A. Ovrut. “Calabi-Yau Metrics for Quotients and Complete Intersections”. In: *JHEP* 05 (2008), p. 080. DOI: 10.1088/1126-6708/2008/05/080. arXiv: 0712.3563 [hep-th].

- [7] Volker Braun, Tamaz Brelidze, Michael R. Douglas, and Burt A. Ovrut. “Eigenvalues and Eigenfunctions of the Scalar Laplace Operator on Calabi-Yau Manifolds”. In: *JHEP* 07 (2008), p. 120. DOI: 10.1088/1126-6708/2008/07/120. arXiv: 0805.3689 [hep-th].
- [8] Matthew Headrick and Ali Nassar. “Energy functionals for Calabi-Yau metrics”. In: *Adv. Theor. Math. Phys.* 17.5 (2013), pp. 867–902. DOI: 10.4310/ATMP.2013.v17.n5.a1. arXiv: 0908.2635 [hep-th].
- [9] Wei Cui and James Gray. “Numerical Metrics, Curvature Expansions and Calabi-Yau Manifolds”. In: *JHEP* 05 (2020), p. 044. DOI: 10.1007/JHEP05(2020)044. arXiv: 1912.11068 [hep-th].
- [10] Anthony Ashmore, Yang-Hui He, and Burt A. Ovrut. “Machine Learning Calabi-Yau Metrics”. In: *Fortsch. Phys.* 68.9 (2020), p. 2000068. DOI: 10.1002/prop.202000068. arXiv: 1910.08605 [hep-th].
- [11] Lara B. Anderson, Mathis Gerdes, James Gray, Sven Krippendorf, Nikhil Raghuram, and Fabian Ruehle. “Moduli-dependent Calabi-Yau and SU(3)-structure metrics from Machine Learning”. In: *JHEP* 05 (2021), p. 013. DOI: 10.1007/JHEP05(2021)013. arXiv: 2012.04656 [hep-th].
- [12] Vishnu Jejjala, Damian Kaloni Mayorga Pena, and Challenger Mishra. “Neural network approximations for Calabi-Yau metrics”. In: *JHEP* 08 (2022), p. 105. DOI: 10.1007/JHEP08(2022)105. arXiv: 2012.15821 [hep-th].
- [13] Anthony Ashmore, Lucille Calmon, Yang-Hui He, and Burt A. Ovrut. “Calabi-Yau Metrics, Energy Functionals and Machine-Learning”. In: *International Journal of Data Science in the Mathematical Sciences* 1.1 (2023), pp. 49–61. DOI: 10.1142/S2810939222500034. arXiv: 2112.10872 [hep-th].
- [14] Magdalena Larfors, Andre Lukas, Fabian Ruehle, and Robin Schneider. “Learning Size and Shape of Calabi-Yau Spaces”. In: (Nov. 2021). arXiv: 2111.01436 [hep-th].
- [15] Magdalena Larfors, Andre Lukas, Fabian Ruehle, and Robin Schneider. “Numerical metrics for complete intersection and Kreuzer-Skarke Calabi-Yau manifolds”. In: *Mach. Learn. Sci. Tech.* 3.3 (2022), p. 035014. DOI: 10.1088/2632-2153/ac8e4e. arXiv: 2205.13408 [hep-th].
- [16] Mathis Gerdes and Sven Krippendorf. “CYJAX: A package for Calabi-Yau metrics with JAX”. In: *Mach. Learn. Sci. Tech.* 4.2 (2023), p. 025031. DOI: 10.1088/2632-2153/acdc84. arXiv: 2211.12520 [hep-th].
- [17] Shamit Kachru, Arnav Tripathy, and Max Zimet. “K3 metrics from little string theory”. In: (Oct. 2018). arXiv: 1810.10540 [hep-th].
- [18] Shamit Kachru, Arnav Tripathy, and Max Zimet. “K3 metrics”. In: (June 2020). arXiv: 2006.02435 [hep-th].
- [19] Seung-Joo Lee and Andre Lukas. “Approximate Ricci-flat Metrics for Calabi-Yau Manifolds”. In: (June 2025). arXiv: 2506.15766 [hep-th].

- [20] Andrei Constantin, Andre Lukas, and Luca A. Nutricati. “Calabi–Yau Metrics with Kähler Moduli Dependence”. In: *arXiv:2603.12384* (Mar. 2026). arXiv: 2603.12384 [hep-th].
- [21] D.D. Joyce. *Compact Manifolds with Special Holonomy*. Oxford mathematical monographs. Oxford University Press, 2000. ISBN: 9780198506010.
- [22] Miles Cranmer. *Interpretable Machine Learning for Science with PySR and SymbolicRegression.jl*. 2023. arXiv: 2305.01582 [astro-ph.IM]. URL: <https://arxiv.org/abs/2305.01582>.
- [23] Viktor Mirjanić and Challenger Mishra. “Symbolic approximations to Ricci-flat metrics via extrinsic symmetries of Calabi–Yau hypersurfaces”. In: *Mach. Learn. Sci. Tech.* 6.3 (2025), p. 035029. DOI: 10.1088/2632-2153/adf68c. arXiv: 2412.19778 [hep-th].